ISSN 0021-3640, JETP Letters, 2021, Vol. 114, No. 8, pp. 441–446. © Pleiades Publishing, Inc., 2021.
Russian Text © The Author(s), 2021, published in Pis'ma v Zhurnal Eksperimental'noi i Teoreticheskoi Fiziki, 2021, Vol. 114, No. 8, pp. 509–514.

OPTICS
AND LASER PHYSICS

Spatial Separation of Scalar Light Beams with Orbital Angular Momentum Using a Phase Metasurface

A. D. Gartman[a, *], A. S. Ustinov[a], A. S. Shorokhov[a], and A. A. Fedyanin[a]

[a] *Faculty of Physics, Moscow State University, Moscow, 119991 Russia*

**e-mail: gartman@nanolab.phys.msu.ru*

Received August 26, 2021; revised September 10, 2021; accepted September 10, 2021

The concept and design optimization of a polarization-independent dielectric metasurface for the spatial separation of scalar light beams with different values of the orbital angular momentum are discussed. The metasurface is based on an array of Mie resonant nanodisks. The geometrical parameters of a structure working at a wavelength of 810 nm are obtained and the displacement of beams with different orbital angular momenta with respect to the axis of the optical system is numerically demonstrated.

DOI: 10.1134/S0021364021200066

Interest in quantum photonics growing in recent years has stimulated the rapid development of the fundamental and applied studies of this field [1]. A number of different platforms and approaches have been proposed, but the most practicable ones seem to be those that can offer a high level of integration and miniaturization within a photonic chip on the micro- and nanoscale, as well as compatibility with the fabrication technologies used in modern microelectronics [2]. The unique properties of such optical devices frequently allow them to surpass the capabilities of bulk analogs (e.g., classical refractive optical elements such as lenses, waveplates, etc.) in controlling nonclassical radiation [3, 4] and offer broad prospects for scaling.

A specific field in quantum photonics, which is of particular interest for the problems of cryptography and computations with nonclassical light, is the study of electromagnetic radiation possessing orbital angular momentum [5]. The latter is the contribution to the angular momentum of a light beam (added to the spin angular momentum) that depends on the field distribution at each point in space. In contrast to spin angular momentum, associated with the polarization of photons and assuming the values of $\pm\hbar$, orbital angular momentum varies in the range from $-l\hbar$ to $l\hbar$ and provides theoretically a greater number of available degrees of freedom, which leads to an increase in the dimension of the Hilbert space [6]. It was demonstrated that the benefits of increased dimension include not only a higher optical data encoding density per channel [7] but also an enhanced security of communication resulting from higher resistance to external interventions [8]. Laguerre–Gaussian scalar light beams represent an example of radiation carrying orbital angular momentum [9], which makes them particularly interesting for quantum cryptography problems [10, 11]. This interest is primarily related to the creation of reliable and secure broadband communication channels for data transmission and processing [12]. However, despite all the advantages of working with light possessing such a large number of degrees of freedom, there have been few devices implemented to date on a compact integrated platform.

In this regard, solutions allowing the control of light carrying orbital angular momentum that are based on new approaches and principles are highly desirable. One of the key tasks in this area is to accomplish the spatial separation of scalar light beams with different values of the orbital angular momentum [13, 14]. This can be achieved using planar optical devices called metasurfaces, which are two-dimensional arrays of resonant nanostructures specially designed to create a complex phase profile [15] for the efficient generation and control of high-dimension entangled quantum states [16].

It was shown recently that the use of metasurfaces based on subwavelength nanoresonators makes it possible to effectively control both classical [17–19] and quantum radiation [20, 21]. In particular, it was demonstrated that, using a metasurface with a special phase profile consisting of cells of silicon nanoparticles, it is possible to measure and reconstruct single- and multiple-photon states of light, with reliable reconstruction of the amplitude, phase, coherence,

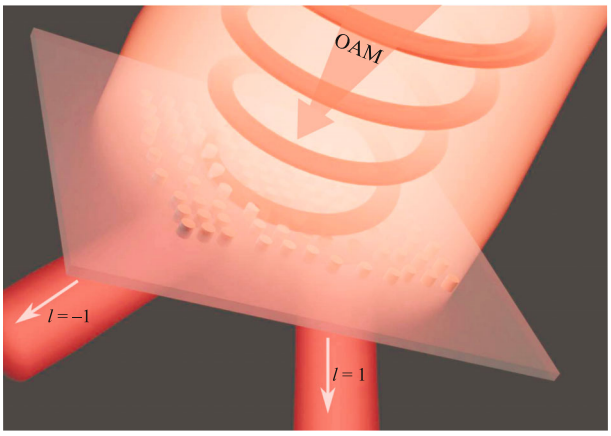

Fig. 1. (Color online) Schematic representation of a resonance silicon metasurface separating scalar beams with different values of the orbital angular momentum (OAM) in space.

and entanglement of states encoded in the polarization of the incident radiation [22].

Here, we consider the spatial separation of scalar beams with orbital angular momentum using resonant silicon metasurfaces with a particular phase profile. The spatial separation of radiation transmitted by a silicon metasurface is depicted schematically in Fig. 1. As a scalar beam carrying different orbital angular momenta passes the metasurface, it undergoes a transformation of its phase and splits into two components corresponding to $l = -1$ and $+1$. As mentioned above [23], silicon metasurfaces are used to solve this problem because of their compact size, ease of manufacturing, and compatibility with modern microelectronics industrial technology [24]. In contrast to the previously presented analogs [14], the silicon metasurface with a complex surface profile proposed here is also polarization independent.

The problem of the spatial separation of radiation carrying different orbital angular momenta has a classical solution [25], which can be described by the following expressions:

$$\phi_1(x,y) = \frac{2\pi a}{\lambda f} \times \left[y \arctan\left(\frac{y}{x}\right) - x \ln\left(\frac{\sqrt{x^2+y^2}}{b}\right) + x \right], \quad (1)$$

$$\phi_2(x,y) = -\frac{2\pi ab}{\lambda f} \exp\left(-\frac{U}{a}\right) \cos\left(\frac{V}{a}\right). \quad (2)$$

These formulas result from the solution of the problem of mapping an object from the (x, y) to (u, v) plane for the case of the transformation from Cartesian to log-polar coordinates: $u = -a \ln(\sqrt{x^2 + y^2}/b)$, $v = a \arctan(y/x)$, where $a = g/2\pi$ (here, g is the transverse size of the transformed beam) and the parameter b is responsible for the shift of the obtained image along the u direction. The first transformation specified by Eq. (1) implements a conformal mapping $(x; y) \to (u; v)$ that converts a beam with a helical phase profile into a laterally elongated beam with a linear phase gradient. If such a beam passes a lens, radiation carrying different orbital angular momenta will be focused at different spots displaced in the lateral direction on the output screen. However, the change in the optical path length that appears upon this transformation implies that the filter described by Eq. (1) introduces a phase distortion in the radiation profile. To correct this distortion and to collimate the beam at the output of the optical system, the phase-correcting transformation described by Eq. (2) has to be applied. It should be noted that the centers of the incident beam and the metasurface have to coincide for performing correct coordinate transformation. This is required for the subsequent effective spatial separation of radiation carrying different orbital angular momenta. Therefore, the helical profile of the phase of incident electromagnetic radiation is changed via two transformations: one for the coordinate conversion and the other for the correction of phase distortions [26].

In order to perform the spatial separation of scalar beams according to different values of the orbital angular momentum with the help of a silicon metasurface, certain conditions on the metasurface phase profile should be satisfied [27]. First, it is necessary to implement such a geometry of the metasurface phase mask that the transmission coefficient is high (as close to 1 as possible) at the selected (working) wavelength and remains constant for the entire range of variations of the geometrical parameters of the structure. Second, it is necessary to ensure that the phase shift of the transmitted electromagnetic radiation can vary in the range from 0 to 2π. Taking into account these requirements, we carried out numerical simulation of the transmission coefficient and the phase of the transmitted wave (Figs. 2a and 2b, respectively) for arrays of silicon nanodisks with a height of $h = 130$ nm and a diameter of $d = 210$ nm. Calculations were performed by the finite-difference time-domain method in the Lumerical FDTD software package. The above values of h and d were chosen because the electric and magnetic dipole resonances overlap in silicon nanodisks with these sizes in the spectral range of interest [28–30]. At a selected wavelength of 810 nm, there exists a range of array periods where the transmittance is very close to unity (Fig. 2c) and the phase of the transmitted wave varies from 0 to 2π (Fig. 2d). This wavelength is chosen because quantum radiation possessing orbital angular momentum is frequently implemented on the basis of a diode laser with a wavelength of 405 nm and a nonlinear crystal (e.g., KTP) in the regime of collinear generation of biphotons [31].

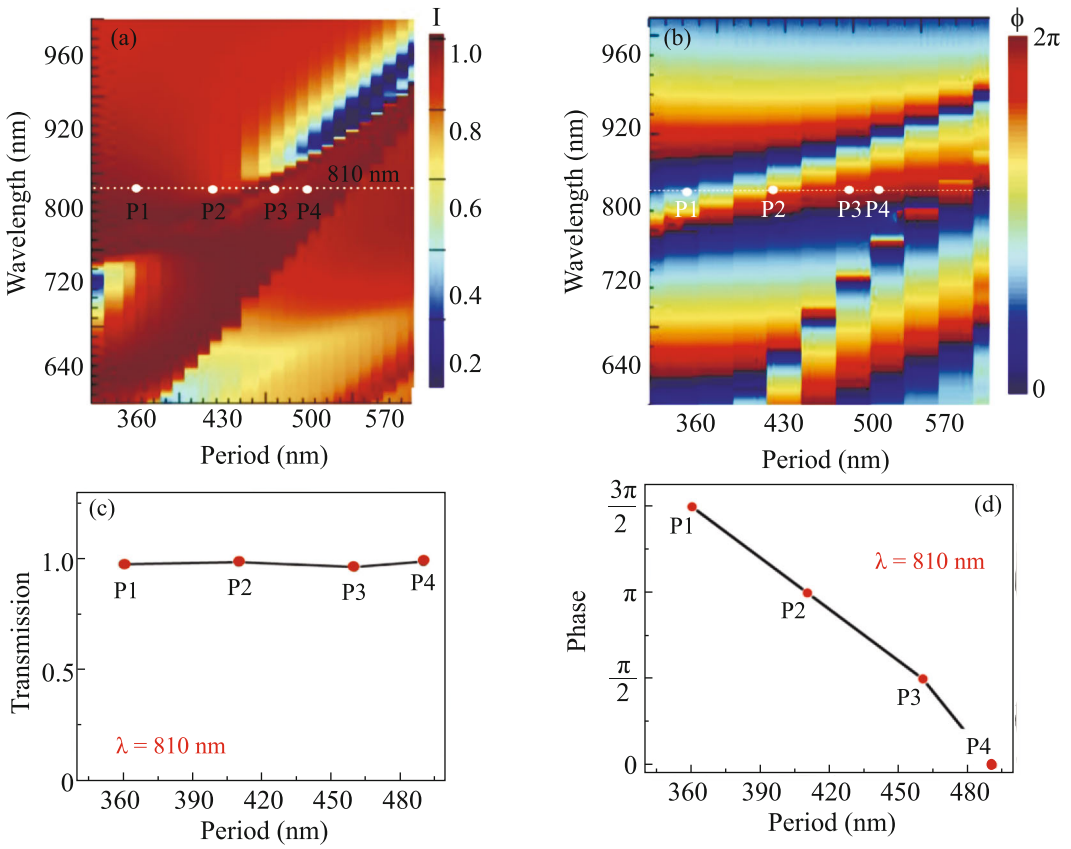

Fig. 2. (Color online) (a, b) Wavelength, array period maps of the (a) transmittance and (b) phase of the transmitted wave for an array of silicon nanodisks with a height of $h = 130$ nm and a diameter of $d = 210$ nm. (c) Transmittance and (d) the phase of the transmitted wave at the selected wavelength of $\lambda = 810$ nm for an array of silicon nanodisks with a height of $h = 130$ nm and a diameter of $d = 210$ nm versus the array period.

The phase mask for the silicon metasurface was designed to realize the transformation given by (1). Figure 3 shows the surface described by Eq. (1) and representing the variation of the phase profile in the range of 0–200π. Calculations were performed for an area of 200 × 200 μm^2 corresponding to the sizes of actual structures. This area was divided into equal parts in the form of 20 × 20-μm squares, and the values of the phase were averaged and normalized to the range of 0–2π within each of these squares. Then, the period of a silicon nanodisk array corresponding to the best possible description of the phase change in each square was determined using previously reported results [32] (Fig. 3b).

Therefore, we devised the optimum design for the required silicon metasurface, which represents a two-dimensional resonant structure divided into square regions with constant phase. Each of these squares consists of an array of silicon nanodisks with a height of $h = 130$ nm, a diameter of $d = 210$ nm, and a period selected according to Table 1.

The described concept of the resonant silicon metasurface design is not the only possible one, but the ease of fabrication makes this solution attractive for experimental realization.

Figure 4 shows the optical setup for the spatial separation of scalar beams carrying orbital angular momentum by a system consisting of the silicon metasurface performing the conformal coordinate mapping and the phase-correcting surface; a spatial light modulator may play the role of the latter. Numerical modeling was performed by solving the Fraunhofer diffraction equations using the physical optics module of the Zemax OpticStudio software package. A scalar beam possessing orbital angular momentum passes a silicon dielectric metasurface, which performs the coordinate transformation. The spatial separation of the incident radiation into spots corresponding to different orbital

Table 1. Correspondence between the phase range and the period of the silicon nanodisk array within the squares of the metasurface

Phase range	0–π/2	π/2–π	π–3π/2	3π/2–2π
Period, nm	360	407	460	493

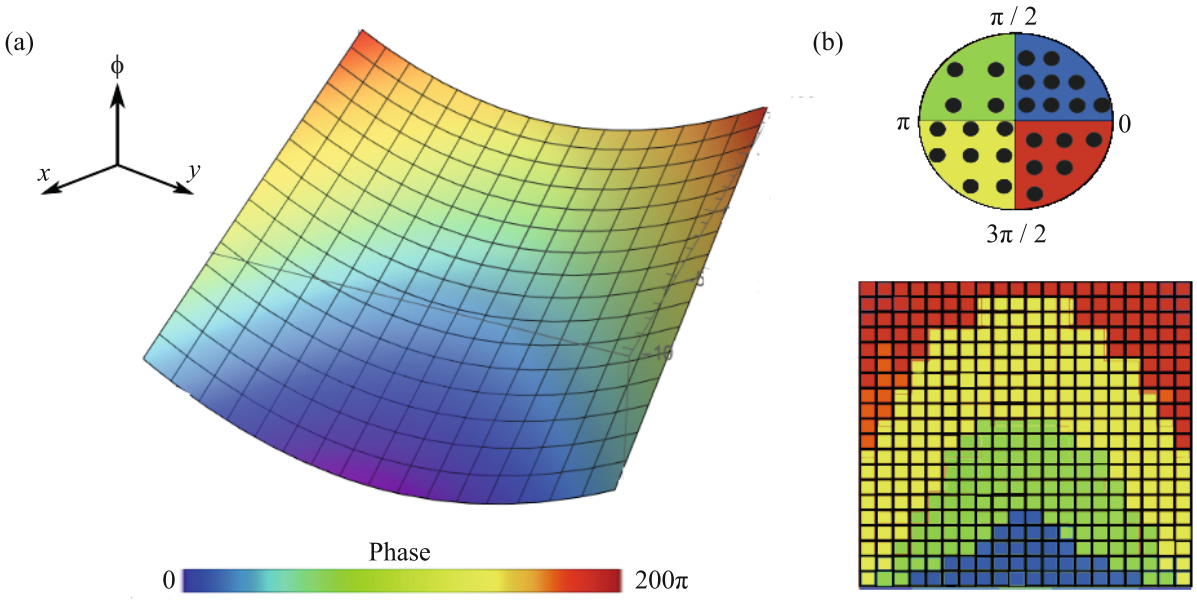

Fig. 3. (Color online) (a) Phase surface determined by transformation (1) and describing the variation of the phase profile in the range of 0–200π. (b) Layout of the phase mask for the silicon metasurface representing an array of 20 × 20-μm squares corresponding to phase ranges of (blue) 0–π/2, (green) π/2–π, (yellow) π–3π/2, and (red) 3π/2–2π.

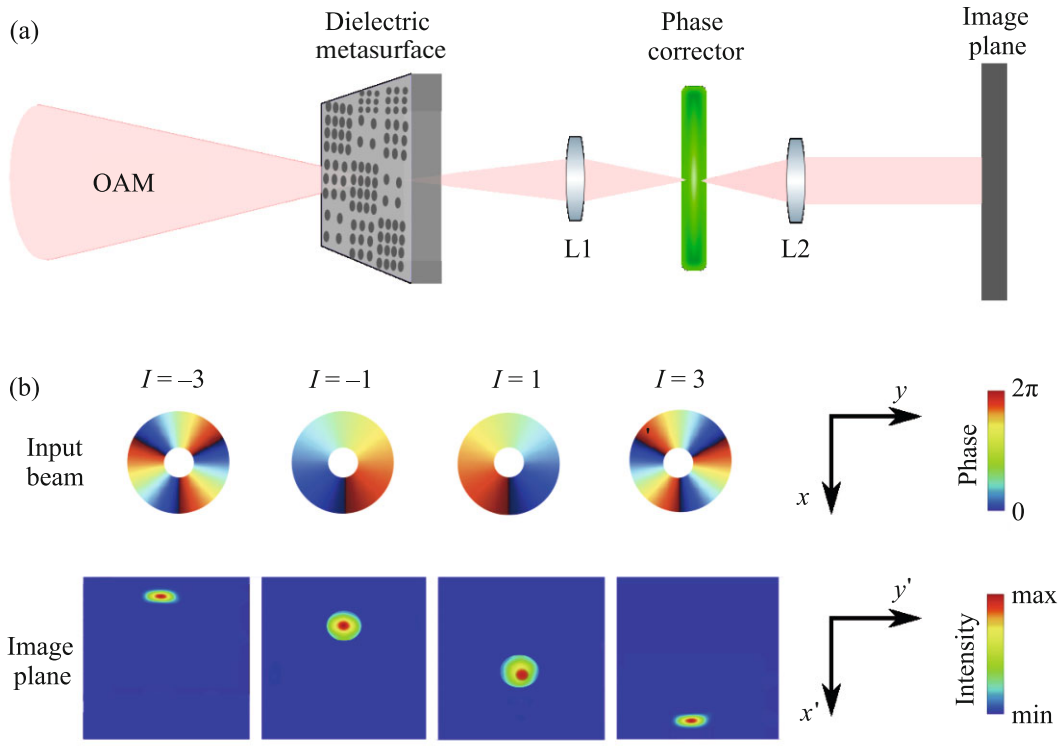

Fig. 4. (Color online) (a) Layout of the optical system for the spatial separation of scalar beams with different orbital angular momenta. (b) Different phase profiles of the input beam and the corresponding spots in the image plane.

angular momentum components is observed on a screen in the image plane. Figure 4b shows the phase profiles of the input beams and the spots in the image plane corresponding to these profiles. Beams with orbital angular momenta $l = \pm 1$ and ± 3 are considered. Similar results can be obtained for other cases, and the above values of l are chosen just for illustrative purposes. The scalar beams of opposite signs are spatially separated with respect to the central optical axis of the system: each value of l is characterized by a localization spot in the $X'Y'$ plane shifted along the Y' coordinate on the opposite sides from zero, depending on the sign and absolute value of the orbital angular momentum. Beams with positive values of the orbital angular momentum $l = 1$ and 3 appear above the OX axis, while beams with $l = -1$ and -3 appear below the OX axis. The components characterized by orbital angular momenta of the same absolute value but opposite signs shift by the same distance in opposite directions.

To summarize, we have used numerical simulations to investigate resonance metasurfaces, i.e., planar optical structures consisting of an array of cylinder silicon nanoparticles featuring high transmittance and providing complete phase control of the transmitted light. We have shown that the use of silicon metasurfaces with a specially selected profile makes it possible to effectively separate in space components of radiation with different orbital angular momenta. The results obtained can be used in quantum cryptography for the development of compact devices for the analysis of nonclassical light.

ACKNOWLEDGMENTS

We are grateful to S.S. Straupe for constructive comments and valuable advice.

FUNDING

This study was supported by the Russian Foundation for Basic Research, project nos. 19-32-90223 (modeling of uniform metasurfaces and optimization of their response) and 20-02-00897 (numerical demonstration of the spatial separation of light beams). Part of the study was supported by the Quantum Technology Center, Moscow State University.

CONFLICT OF INTEREST

The authors declare that they have no conflicts of interest.

REFERENCES

1. S. Slussarenko and G. Pryde, Appl. Phys. Rev. **6**, 041303 (2019).
2. J. Wang, F. Sciarrino, A. Laing, and M. Thompson, Nat. Photon. **14**, 273 (2020).
3. F. Peyskens, C. Chakraborty, M. Muneeb, D. Thourhout, and D. Englund, Nat. Commun. **10**, 4435 (2019).
4. A. D. Gartman, M. K. Kroychuk, A. S. Shorokhov, and A. A. Fedyanin, JETP Lett. **112**, 693 (2020).
5. L. Allen, M. Beijersbergen, R. Spreeuw, and J. Woerdman, Phys. Rev. **45**, 8185 (1992).
6. D. Andrews and M. Babiker, *The Angular Momentum of Light* (Cambridge Univ. Press, Cambridge, UK, 2012).
7. M. Mirhosseini, O. Magana-Loaiza, M. O'Sullivan, B. Rodenburg, M. Malik, M. Lavery, M. Padgett, D. Gauthier, and R. Boyd, New J. Phys. **17**, 033033 (2015).
8. J. O'Brien, A. Furusawa, and J. Vuckovic, Nat. Photon. **10**, 687 (2009).
9. R. Devlin, A. Ambrosio, N. Rubin, J. Mueller, and F. Capasso, Science (Washington, DC, U. S.) **17**, 896 (2017).
10. J. Wang, Photon. Res. **4**, 251 (2016).
11. K. A. Balygin, V. I. Zaitsev, A. N. Klimov, A. I. Klimov, S. P. Kulik, and S. N. Molotkov, JETP Lett. **105**, 606 (2017).
12. X. Wang, Z. Nie, Y. Liang, J. Wang, T. Li, and B. Jia, Nanophotonics **7**, 1533 (2018).
13. M. Mirhosseini, M. Malik, Z. Shi, and R. Boyd, Nat. Commun. **4**, 2781 (2013).
14. G. Ruffato, P. Capaldo, M. Massari, E. Mafakheri, and F. Romanato, Opt. Express **27**, 15750 (2019).
15. S. Pachava, R. Dharmavarapu, A. Vijayakumar, S. Jayakumar, A. Manthalkar, A. Dixit, N. Viswanathan, B. Srinivasan, and S. Bhattacharya, Opt. Eng. **4**, 041205 (2019).
16. F. Yue, D. Wen, C. Zhang, B. Gerardot, W. Wang, S. Zhang, and X. Chen, Adv. Mater. **29**, 1603838 (2017).
17. A. Kuznetsov, A. Miroshnichenko, M. Brongersma, Y. Kivshar, and B. Lukyanchuk, Science (Washington, DC, U. S.) **354**, 6314 (2016).
18. N. Yu and F. Capasso, Nat. Mater. **13**, 139 (2014).
19. S. Kruk, B. Hopkins, I. Kravchenko, A. Miroshnichenko, D. Neshev, and Y. Kivshar, APL Photon. **1**, 030801 (2016).
20. T. Stav, A. Faerman, E. Maguid, D. Oren, V. Kleiner, E. Hasman, and M. Segev, Science (Washington, DC, U. S.) **361**, 1101 (2018).
21. A. S. Solntsev, G. S. Agarwal, and Y. S. Kivshar, Nat. Photon. **15**, 327 (2021).
22. K. Wang, G. Titchener, S. Kruk, L. Xu, H. Chung, M. Parry, I. Kravchenko, Y. Chen, A. Solntsev, Y. Kivshar, D. Neshev, and A. Sukhorukov, Science (Washington, DC, U. S.) **12**, 1104 (2018).
23. H. Hsiao, C. Chu, and D. Tsai, Small Methods **1**, 1600064 (2017).
24. E. Maguid, I. Yulevich, M. Yannai, V. Kleiner, M. Brongersma, and E. Hasman, Light Sci. Appl. **6**, 31031 (2017).

25. O. Bryngdahl, J. Opt. Soc. Am. **64**, 1092 (1974).

26. G. Berkhout, M. Lavery, J. Courtial, M. Beijersbergen, and M. Padgett, Phys. Rev. Lett. **105**, 153601 (2010).

27. K. Chong, I. Staude, A. James, J. Dominguez, S. Liu, S. Campione, G. Subramania, T. Luk, M. Decker, D. Neshev, I. Brener, and Y. Kivshar, Nano Lett. **5**, 5369 (2015).

28. E. V. Melik-Gaykazyan, K. L. Koshelev, J. H. Choi, S. S. Kruk, A. A. Fedyanin, and Y. S. Kivshar, JETP Lett. **109**, 131 (2019).

29. M. K. Kroychuk, D. F. Yagudin, A. S. Shorokhov, D. A. Smirnova, I. I. Volkovskaya, M. R. Shcherbakov, G. Shvets, Y. S. Kivshar, and A. A. Fedyanin, Adv. Opt. Mater. **7**, 1900447 (2019).

30. M. K. Kroychuk, A. S. Shorokhov, D. F. Yagudin, D. A. Shilkin, and A. A. Fedyanin, Nano Lett. **20**, 3471 (2020).

31. E. Kovlakov, S. Straupe, and S. Kulik, Phys. Rev. A **98**, 060301 (2018).

32. K. Chong, L. Wang, I. Staude, A. James, J. Dominguez, S. Liu, G. Subramania, M. Decker, D. Neshev, I. Brener, and Y. Kivshar, ACS Photon. **3**, 514 (2016).

Translated by M. Skorikov